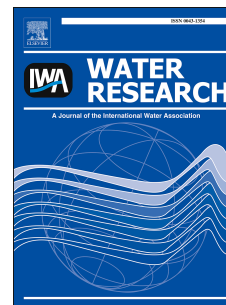# Accepted Manuscript

Efficient treatment of perfluorohexanoic acid by nanofiltration followed by electrochemical degradation of the NF concentrate

Álvaro Soriano, Daniel Gorri, Ane Urtiaga

Please cite this article as: Soriano, E., Gorri, D., Urtiaga, A., Efficient treatment of perfluorohexanoic acid by nanofiltration followed by electrochemical degradation of the NF concentrate, *Water Research* (2017), doi: 10.1016/j.watres.2017.01.043.

This is a PDF file of an unedited manuscript that has been accepted for publication. As a service to our customers we are providing this early version of the manuscript. The manuscript will undergo copyediting, typesetting, and review of the resulting proof before it is published in its final form. Please note that during the production process errors may be discovered which could affect the content, and all legal disclaimers that apply to the journal pertain.
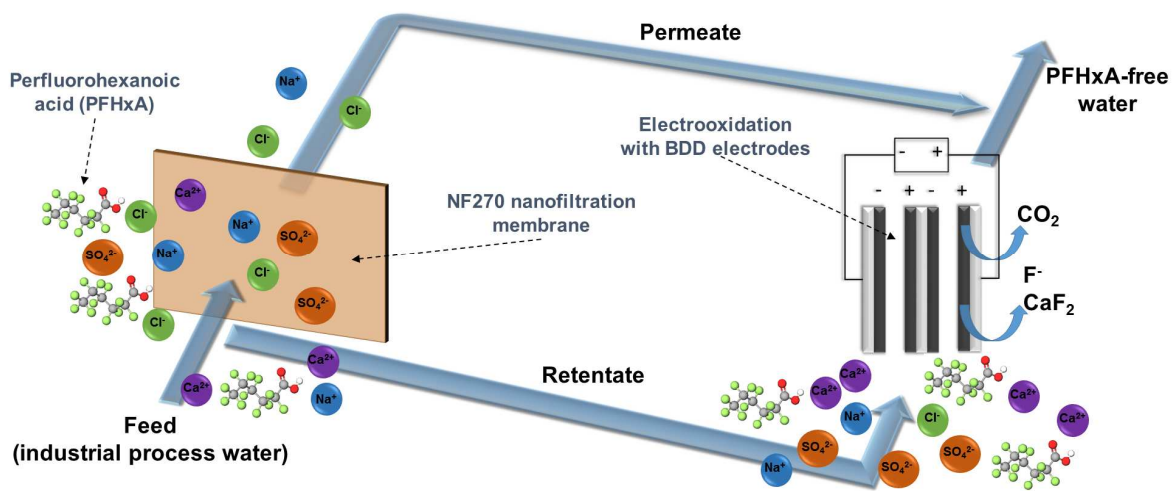
1

2

3 **Efficient treatment of perfluorohexanoic acid by nanofiltration**

4 **followed by electrochemical degradation of the NF concentrate**

5

6 Álvaro Soriano, Daniel Gorri, Ane Urtiaga*

7

8 Department of Chemical and Biomolecular Engineering, University of Cantabria

9 Av. de Los Castros s/n. 39005 Santander. Spain

10 *Corresponding author: urtiaga@unican.es

11

12

13 Revised manuscript

14 Submitted to *Water Research*

15

16 January 2017

17

18

19 **Abstract**

20 The present study was aimed at the development of a strategy for removing and

21 degrading perfluorohexanoic acid (PFHxA) from industrial process waters at

22 concentrations in the range 60-200 $mg \cdot L^{-1}$. The treatment train consisted of

23 nanofiltration (NF) separation followed by electrochemical degradation of the NF

24 concentrate. Using a laboratory-scale system and working in the total recirculation

25 mode, the DowFilm NF270 membrane provided PFHxA rejections that varied in the

26 range 96.6 to 99.4% as the operating pressure was increased from 2.5 to 20 bar. The NF

27 operation in concentration mode enabled a volume reduction factor of 5 and increased

28 the PFHxA concentration in the retentate to 870 $mg \cdot L^{-1}$. Results showed that the

29 increase in PFHxA concentration and the presence of calcium sulfate salts did not

30 induce irreversible membrane fouling. The NF retentate was treated in a commercial

31 undivided electrochemical cell provided with two parallel flow-by compartments

32 separated by bipolar boron doped diamond (BDD) electrode, BDD counter anode, and

33 counter cathode. Current densities ranging from 20 to 100 $A \cdot m^{-2}$ were examined. The

34 electrochemical degradation rate of PFHxA reached 98% and was accompanied by its

35 efficient mineralization, as the reduction of total organic carbon was higher than 95%.

36 Energy consumption, which was 15.2 $kWh \cdot m^{-3}$ of treated NF concentrate, was

37 minimized by selecting operation at 50 $A \cdot m^{-2}$. While most of the previous research on

38 the treatment of perfluoroalkyl substances (PFASs) focused on the removal of

39 perfluorooctanoic acid (PFOA) and perfluorooctane sulfonate (PFOS), these compounds

40 have been phased out by chemical manufacturers. Our findings are relevant for the

41 treatment of PFHxA, which appears to be one of the present alternatives to long-chain

42 PFASs thanks to its lower bioaccumulative potential than PFOA and PFOS. However,

43 PFHxA also behaves as a persistent pollutant. Moreover, our results highlight the

44 potential of combining membrane separation and electrochemical oxidation for the

45 efficient treatment of PFAS-impacted waters.

46 **Keywords:** Perfluorohexanoic acid, perfluoroalkyl substances (PFASs), nanofiltration,

47 electrooxidation, boron doped diamond electrode

48

49 **1. Introduction**

50 Perfluoroalkyl substances (PFASs) are highly persistent organic compounds that

51 contain a fluorinated alkyl chain and a hydrophilic end group (Arvaniti and Stasinakis,

52 2015). PFASs have been used in a wide variety of applications as part of surfactants,

53 emulsifiers, aqueous film forming foams, additives for polymers, for paper and

54 cardboard coatings used in food packaging products, and for stain and water repellency

55 in textiles and leather, among others (Appleman et al., 2014; Rahman et al., 2014; Yu et

56 al., 2009).

57 Long-chain PFASs are bioaccumulative and toxic to laboratory animals and

58 wildlife (ECHA, 2014; Lin et al., 2014). Hence, environmental protection institutions

59 have established limits to perfluoroalkyl carboxylic acids (PFCAs) and perfluoroalkane

60 sulfonates with eight or more fluorinated carbons. Perfluorooctane sulfonate (PFOS)

61 and its salts were added to Annex B of the list developed in 2009 as a result of the

62 Stockholm Convention on Persistent Organic Pollutants (Ahrens and Bundschuh, 2014).

63 PFOS and its derivatives were recently added as priority hazardous substances in

64 Directive 2013/39/UE of the European water policy. The United States Environmental

65 Protection Agency has recently set health advisory levels for perflourooctanoic acid

3

66 (PFOA) and PFOS in drinking water at 0.07 µg/L, both individually and combined

67 (USEPA, 2016).

68   Nowadays, industry has phased out the use of PFOA, PFOS, and longer chain

69 homologues (USEPA, 2015). The alternatives are mostly short chain PFASs such as the

70 6:2 fluorotelomer alcohol (6:2 FTOH), which contains six fully fluorinated carbon

71 atoms (ECHA, 2014). 6:2 FTOH is readily biodegradable, but it degrades into the

72 persistent compounds perfluorohexanoic acid (PFHxA) and perfluoropentanoic acid (L.

73 Zhao et al., 2013). In general, shorter chain PFASs have been reported to be quickly

74 eliminated in mammals (Z. Wang et al., 2015), although PFHxA is equally persistent

75 and cannot be degraded under biotic or abiotic conditions.

76   Various technologies have been examined for the treatment of PFASs from

77 aqueous media, although most of the previous studies were exclusively focused on the

78 removal of PFOA and PFOS. The most widely studied techniques are adsorption,

79 membranes, and oxidation processes (Arvaniti and Stasinakis, 2015). The use of

80 activated carbon and anion exchange resins was successfully reported for the retention

81 of PFOA and PFOS (Yu et al., 2009; Zaggia et al., 2016; Zhang et al., 2016).

82 Nanofiltration (NF) and reverse osmosis (RO) processes are of special interest in the

83 separation of PFASs from drinking water sources. Several works studied the rejection of

84 PFASs by NF membranes, which ranged from 90% to 99%. Rejections were mainly

85 dependent on the type of membrane, but also on a variety of other factors that included

86 the properties of the solution and the effect of the operating variables (Appleman et al.,

87 2013; Hang et al., 2015; Steinle-Darling and Reinhard, 2008; Tang et al., 2007; T.

88 Wang et al., 2015; C. Zhao et al., 2013). Other studies reported that RO could achieve

89 higher PFASs rejection than NF, which in most cases was better than 99%, but at the

90 expense of significantly lower permeate fluxes (Baudequin et al., 2014; Tang et al.,

91   2007, 2006). Only a few studies included data about PFHxA rejections by the NF270

92   membrane (Steinle-Darling and Reinhard, 2008). It is important to note that those

93   studies used artificial or spiked mixtures of PFASs that included PFHxA in low

94   concentrations (1 µg·L^{-1} and 100-400 ng·L^{-1}), and thus may not reflect mechanisms that

95   dominate at higher PFHxA concentrations similar to those usually found in industrial

96   process streams. Moreover, PFHxA rejection values (> 95%) reported by Appleman et

97   al. (2013) were estimations, as the permeate concentrations were not quantified due to

98   limitations of the analytical technique in the low permeate concentration range.

99   The use of membrane processes alone is not enough for the overall treatment of

100   PFASs because these compounds are retained in the concentrate stream, which must be

101   treated before disposal. Although the concept of coupling membrane technology with

102   advanced oxidation processes has been previously reported in the treatment of emerging

103   micropollutants such as pharmaceutical compounds in a wide variety of water samples

104   (Dialynas et al., 2008; Ioannou et al., 2013; Pérez et al., 2010; Radjenovic et al., 2011),

105   we are unaware of any studies assessing the impact of its application to the treatment of

106   PFASs.

107   The strength of the C-F bond makes PFASs resistant to traditional advanced

108   oxidation processes (Sansotera et al., 2014). Electrochemical treatment by anodic

109   oxidation has been examined by several research groups (Chaplin, 2014). Boron doped

110   diamond (BDD) electrodes could satisfactorily decompose the PFOA and PFOS

111   contained in synthetic water solutions (Carter and Farrell, 2008; Ochiai et al., 2011;

112   Urtiaga et al., 2015). BDD electrodes have interesting properties that make their use

113   advantageous for the treatment of organic pollutants. These are their high chemical

114   inertness, hardness, extended lifetime, the ability to generate hydroxyl radicals (HO$^{\bullet}$)

115   from water oxidation, and the efficient use of electrical energy (Cañizares et al., 2005;

116   Cabeza et al., 2007; Polcaro et al., 2009; Pérez et al., 2010). Most of the research effort

117   is currently focused on the development of new electrode materials (Xue et al., 2015;

118   Yang et al., 2015; H. Zhao et al., 2013; Zhuo et al., 2014) and very little information is

119   available about the electrochemical degradation of PFASs in real polluted water

120   matrixes. Exceptions include the recent study by Schaefer et al. (2015), who

121   demonstrated the electrochemical degradation of PFOA and PFOS in groundwater

122   impacted by the use of aqueous film-forming foams. It is noted that the majority of

123   previous studies have focused exclusively on the removal of PFOA and PFOS. One

124   notable gap is the lack of knowledge about the electrochemical treatment of shorter-

125   chain PFASs that are used in chemical manufacturing processes as alternatives to PFOA

126   and PFOS.

127   The objective of this work was to study the removal of PFHxA from two process

128   waters produced in an industrial manufacturing process in which the initial

129   concentration of PFHxA was in the range 60-200 mg·L^{-1}. The treatment train began

130   with an initial nanofiltration separation that allowed concentration of PFHxA within the

131   retentate stream. This was subsequently degraded by electrooxidation using BDD

132   electrodes. A commercial BDD electrochemical cell was used. The study of the

133   operating variables that affected the rejection of PFHxA and other salts contained in the

134   process waters was assessed. The effect of the applied current and the mechanisms that

135   govern the kinetics of the electrochemical process are also discussed.

136

137   **2. Materials and methods**

138   *2.1 Water characteristics*

139   Two different samples of process streams produced in an industrial

140   manufacturing process were used in this experimental work. The samples were taken

141   just before the PFHxA collecting facility that removed the contaminant before the

142   general wastewater treatment was applied at the industrial plant. Table 1 displays the

143   chemical characterization of the two samples, referred to as S1 and S2. The main

144   difference lays in the content of PFHxA, which is about three times higher in S1 than in

145   S2. Other components were common inorganic salts, which provided the samples the

146   adequate conductivity for use as an electrolyte in the electrochemical experiments. It

147   can be noticed that the values of total organic carbon (TOC) exceeded the theoretical

148   TOC values calculated from the concentration of PFHxA. Therefore, the industrial

149   waters contained other soluble organic compounds of unknown nature.

150   In additional to the real process waters described above, model solutions with

151   salt contents equivalent to the real ones were prepared. All chemicals were of analytical

152   grade and used as received without further purification. Perfluorohexanoic acid ($\geq$ 97%)

153   was supplied by Sigma-Aldrich. Calcium sulfate dihydrate ($\geq$ 98%) was purchased from

154   Scharlau. Sodium chloride ($\geq$ 99%) was obtained from Panreac. Sodium carbonate ($\geq$

155   99.9%) was supplied by Merck Millipore.

156   *2.2 Nanofiltration experiments*

157   Nanofiltration experiments were carried out in a laboratory membrane cross-

158   flow test cell (SEPA-CF, GE Osmonics). An NF270 flat membrane supplied by Dow

159   Filmtec was used. It is a thin film composite of a polyester non-woven support matrix, a

7

160   microporous polysulfone interlayer, and a semiaromatic piperazine-based aromatic

161   polyamide barrier layer. At neutral pH, the NF270 membrane surface is negatively

162   charged, a property that would improve the rejection of large negative species such as

163   perfluorohexanoate, which is obtained by the dissociation of PFHxA at neutral pH

164   (Wang et al., 2016).

165   The membrane area inside the cell was 155 cm^2. New membrane specimens

166   were preconditioned by immersion in ultrapure water for 24 h to 48 h. A back pressure

167   valve (Swagelok, 0-40 bar), installed at the outlet port of the retentate stream, was used

168   to control the operating pressure. The permeate chamber was maintained at atmospheric

169   pressure. The feed was circulated using a diaphragm pump (Hydra-Cell D-03).

170   Fig. 1 shows the NF set-up. In the total recirculation experiments (Fig. 1a), both

171   the retentate and the permeate streams were continuously recycled to the feed tank.

172   Therefore, in the total recirculation NF experiments the feed composition was constant

173   during the entire experiment. Initially, the NF system was pressurized with the feed

174   solution at 20 bar for one hour with total recirculation of the solution. After achieving

175   stable permeate fluxes in consecutive measurements for at least one hour, the pressure

176   was sequentially reduced to 15, 10, 5, and 2.5 bar. At each pressure, the system was

177   allowed to reach steady-state flux before the next reduction in operating pressure. In

178   concentration mode experiments (Fig. 1b), only the rejection stream was recycled to the

179   feed tank, while the permeate stream was collected in a separate tank. In concentration

180   mode experiments, the concentration of PFHxA and salts in the feed continuously

181   increased during the length of the experimental run. Concentration mode experiments

182   were conducted until a volume reduction factor (VRF) approximately equal to 5 was

183   obtained, where VRF is defined as the ratio between the initial feed volume and the

184   concentrate final volume (Mulder, 1996). In concentration mode, the membrane was

185   initially pressurized for one hour at 35 bar using deionized water. The pressure was then

186   fixed at 10 bar during the NF test. In all experiments, the permeate rejection and feed

187   streams were sampled periodically. All experiments were conducted at room

188   temperature.

189   *2.3 Electrooxidation experiments*

190   The retentate stream produced in the NF concentration mode tests, which

191   accumulated PFHxA and soluble salts, was used as the feed solution in the

192   electrooxidation experiments. The set-up consisted of an electrochemical cell (DiaCell

193   201 PP, Adamant Technologies), a power supply (Vitecom 75-HY3005D), a jacketed

194   feed tank, and a cooling bath (Polyscience 9510). The cell contained two parallel flow-

195   by compartments made of a central bipolar p-Si/BDD electrode and p-Si/BDD anode

196   and cathode, with an interelectrode gap of 1 mm in each channel. Further details on the

197   experimental system can be found elsewhere (Díaz et al., 2011; Urtiaga et al., 2014).

198   The feed tank was filled with 1 L of the NF concentrate, unless otherwise stated. The

199   experiments were carried out in batch mode, at a constant temperature of 20 °C. Three

200   different current densities were applied: 20, 50, and 100 A·m^{-2}. Model solutions

201   representative of the NF concentrates were used in the experiments aimed at the

202   selection of the optimum operating conditions for electrooxidation.

203   To determine the efficiency of the process, it is useful to calculate the specific

204   electrical charge (Q, A·h·L^{-1}) and the energy consumption (W, kWh·m^{-3}) as follows

205   (Anglada et al., 2009):

$$Q = \frac{JAt}{v} \tag{1}$$

$$W = QV \tag{2}$$

206 where J is the current density (A·m^{-2}), A is the total anode area (m^2), t is the time (h), v

207 is the feed tank volume (L), and V is the cell voltage (V).

208   The limiting current density (J_{lim}, A·m^{-2}) at a given time t, can be calculated as

209 follows (Martínez-Huitle et al., 2015; Panizza and Cerisola, 2009):

$$J_{lim} = 12Fk_m[PFHxA]_t \tag{3}$$

211 where F is the Faraday constant (C·mol^{-1}), $[PFHxA]_t$ is the concentration of PFHxA

212 (mol·m^{-3}) at a given experimental time, and k_m is the mass transport coefficient in the

213 electrochemical reactor (m·s^{1}). The factor of 12 is the number of electrons exchanged

214 during the oxidation of one PFHxA molecule. k_m was calculated following the work of

215 Anglada et al. (2010), who analyzed the effect of hydrodynamics and scale-up for

216 electrochemical cells with a similar geometry to the equipment used in the present

217 study.

218 *2.4 Analytical methods*

219   The perfluorinated compounds were quantified using two different analytical

220 methods. The appropriate method was selected according to the PFHxA concentration

221 range and to the calcium and bicarbonate content in the samples:

222   1. The PFHxA concentration in the feed and retentate NF samples was generally

223   within the range 5-900 mg·L^{-1}. Moreover, these samples had high calcium,

224   sulfate, and bicarbonate concentrations. High-performance liquid

225   chromatography (HPLC) with a diode array UV-visible detector was employed

226   (Waters 2695-DAD). The separation column was an X-Bridge C18 (5 μm, 250

227   × 4.6 mm). The mobile phase was a solution of methanol (CH_3OH) and sodium

228   dihydrogen phosphate ($Na_2H_2PO_4$, 20 mM) in the 65:35 volume ratio at a flow

229   rate of 0.5 mL·min^{-1}. The limit of quantification (LOQ) for PFHxA was 5 mg·L^{-1}

230   . The UV absorption at 205.4 nm was used for quantification.

231   2. HPLC (Waters 2690) equipped with a triple quadrupole mass spectrometer

232   (TQD Detector Acquity, Waters) was used to analyze NF permeate samples,

233   with PFHxA concentrations generally below 5 mg·L^{-1} and with low salt content.

234   The column was the X-Bridge BEH C18 (2.5 μm, 2.1 × 75 mm). The eluents

235   were: (i) an aqueous solution containing ammonium acetate ($CH_3COOHNH_4$) 2

236   mM and 5% of methanol, and (ii) pure methanol. The eluent flow rate was 0.15

237   mL·min^{-1}. The LOQ for PFHxA was 1 μg·L^{-1}.

238   It was checked that both analytical protocols provided analogous PFHxA

239   quantification in the feed sample S1.

240   Conductivity was measured using a portable conductivity meter (Hach sensION

241   5). The pH was measured using a pH meter (GLP Crison 22). An automatic carbon

242   analyzer (TOC-V CPH Shimadzu) was used to measure the total organic carbon (TOC).

243   The determination of chloride, sulfate, and fluoride anions was carried out by ion

244   chromatography (Dionex ICS-1100) using an ion exchange resin column (Dionex AS9-

245   HC). The mobile phase was sodium carbonate (Na_2CO_3, 9 mM) with a flow rate of 1

246   mL min^{-1}. Sodium and calcium cations were determined by ion chromathography

247   (Dionex DX-120) using a Dionex IonPac TM CS12 column and methanesulfonic acid

248   (18 mM at 1 mL min^{-1}) as eluent.

11

249   **3. Results and discussion**

250   *3.1 Nanofiltration experiments*

251   *3.1.1 Total recirculation tests*

252   The volumetric flux of permeate passing through the membrane, J_v, is defined

253   by Darcy's law (Eq. (4)), which states that this variable is the product of the membrane

254   permeability L_p (L·m^{-2}·h^{-1}·bar^{-1}), which is an empirical constant, and the pressure

255   gradient between the two sides of the membrane, defined as the difference between the

256   effective pressure ΔP (bar) and the osmotic pressure gradient $\Delta \pi$ (bar) (Pérez-González

257   et al., 2015):

$$J_v = L_p(\Delta P - \Delta \pi) \tag{4}$$

258   where $\Delta \pi$ is defined as:

$$\Delta \pi = \pi_0 - \pi_p \tag{5}$$

259   where π_0 and π_p are the feed and the permeate osmotic pressures, respectively. The

260   osmotic pressure of the solutions was calculated from the concentration of the dissolved

261   salts (Asano, 1998):

$$\pi = 1.19 \, (T + 273) \sum m_i \tag{6}$$

262   where T is the temperature of the solution (ºC) and m_i is the molality of the constituent

263   in the solution.

264   Fig. 2 shows the correlation between the permeate flux and the pressure gradient

265 across the membrane. Three types of water samples were considered: ultrapure water,

266 real industrial process waters, and the model solution. The last represents the salt

267 composition of the real samples S1 and S2, according to Table 1, but without the

268 addition of PFHxA. It was observed that the membrane permeability to ultrapure water

269 was highest, L_{pw}=13.3 ± 0.04   L·m^{-2}·h^{-1}·bar^{-1}, a value that is similar to previously

270 reported water permeabilities for the same NF270 membrane (Nghiem and Hawkes,

271 2007). The presence of salts in solution decreased the membrane permeability, as was

272 observed for the flux data obtained with the model solution, L_{pm}= 11.7 ± 1.2 L·m^{-2}·h^{-}

273 ^{1}·bar^{-1}. A similar trend was observed in previous studies dealing with the NF treatment

274 of desalination brines, e.g., Pérez-González et al. (2015) found that solution

275 permeability decreased exponentially when increasing the initial salt concentration. The

276 membrane permeabilities of the two samples of real process water S1 and S2 (which

277 contained PFHxA) were very similar to each other ($L_{p,S1}$=9.6 L·m^{-2}·h^{-1}·bar^{-1}, and $L_{p,S2}$=

278 9.4 L·m^{-2}·h^{-1}·bar^{-1}), and lower than the values for pure water and the model salt solution.

279 Hang et al. (2015) reported a similar observation after the nanofiltration of PFOA and

280 suggested that such behavior could be attributed to adsorption of the molecule in the

281 expanded membrane pores.

282   The effect of the effective pressure gradient on the rejection of PFHxA and ions

283 was also studied. The observed rejection (R_{obs}) was calculated as follows (IUPAC,

284 1996):

$$R_{obs} = \left(1 - \frac{c_p}{c_r}\right) \times 100 \tag{7}$$

13

285   where C_p and C_r are the concentration of the species in the permeate and retentate

286   streams, respectively.

287   Due to the high solvent flow through the membrane and the high rejection of the

288   species, solutes accumulated on the membrane surface. Thus, the actual solute

289   concentration at the membrane surface was higher than in the bulk solution, known as

290   the concentration polarization phenomenon. In order to calculate the real membrane

291   rejections (R_{real}) the equation of Fujioka et al. (2012) was employed:

$$R_{real} = \frac{R_{obs} \exp\left(\frac{J_v}{k}\right)}{1 + R_{obs}\left[exp\left(\frac{J_v}{k}\right) - 1\right]} \times 100 \qquad (8)$$

292   where k is the mass transfer coefficient of the considered species (m·s^{-1}). k was

293   calculated using Eq. (9), which is valid for laminar flow through rectangular closed

294   channels (van den Berg et al., 1989):

$$Sh = \frac{2hk}{D_{AB}} = 0.664 \cdot Re^{0.5} Sc^{0.33} \left(\frac{2h}{L}\right)^{0.33} \qquad (9)$$

295   In Eq. (9) Sh, Re, and Sc are the Sherwood, Reynolds, and Schmidt numbers,

296   respectively; h is the NF cell channel height (1.7 mm) and L is the length of the path

297   that follows the fluid inside the NF cell (0.13 m). D_{AB} is the diffusion coefficient of the

298   species in water (m^2·s^{-1}). The diffusion coefficients reported by Samson et al. (2003)

299   were applied for the ionic species (sulfate, calcium, sodium, and chloride). In the case of

300   PFHxA, the Wilke-Chang equation (Perry et al., 1997) was used to estimate its

301   diffusion coefficient in water, $D_{PFHxA,w}$=7.05×10^{-10} m^2·s^{-1}, at 25°C.

302   The dependence of the PFHxA real rejection on the effective pressure is shown

303   in Fig. 3. The PFHxA rejection increased from 97.3% to 99.1% for S1, and from 96.6%

304   to 99.4% for S2 in the range of effective pressure gradient $2.4 < (\Delta P - \Delta \pi) < 19.9$ bar.

305   Two main observations can be derived. First, the PFHxA real rejection remained high

306   over the entire range of applied pressure. Secondly, the difference in the concentration

307   of PFHxA, which was three times higher in S1 than in S2, did not significantly affect

308   the rejection percentage. Appleman et al. (2013) reported PFHxA rejections higher than

309   95%, when using the same NF270 membrane for the treatment of spiked artificial

310   groundwater with a feed PFHxA concentration of 1 $\mu g \cdot L^{-1}$. The authors revealed that

311   PFHxA was not detected in the permeate over the limit of quantification of the

312   analytical technique used in that work. It can be argued that the differences in the feed

313   concentration, which in the study of Applemann et al. (2013) was 200 times lower than

314   in sample S1 of the present study, significantly reduced the concentration gradient

315   across the membrane and thus the permeation flux of the species. Similar observations

316   were reported by Steinle-Darling and Reinhard (2008) who studied the nanofiltration of

317   synthetic mixtures of 15 perfluorochemicals in deionized water with concentrations in

318   the range 150-400 $ng \cdot L^{-1}$. So far, to the best of our knowledge, the present study is the

319   first one reporting the NF of PFHxA in real industrial process waters. Past research

320   (Bellona and Drewes, 2007) demonstrated that NF membranes achieved a high rejection

321   of negatively charged organic compounds through electrostatic exclusion. However, the

322   detection of PFHxA in the permeate observed in the present work suggests that once the

323   compound reached a partitioning equilibrium at the feed/membrane interface—which is

324   enhanced by the high feed concentrations used in this work—the diffusion mechanism

325   governs the overall solute transport through the membrane pores.

326   Fig. 4 shows the real rejection of ions (sulfate, chloride, sodium, and calcium) as

327   a function of the operating pressure for the sample S1. Similar rejections were observed

328   when NF was applied to S2 and to the model solutions (results not shown). In the range

329   of operating pressures studied, chloride rejection increased from 6.8% to 56.4%, sodium

330   rejection from 65.6% to 88.2%, calcium rejection from 87.3% to 97.9%, and sulfate

331   rejection from 98.8% to 99.6%. The high values of sulfate rejection are very similar to

332   those obtained for PFHxA because both are large negatively charged species that are

333   easily rejected by the negatively charged membrane at neutral pH. The low value of

334   chloride rejection can be explained by the Donnan ion distribution between the solution

335   and the membrane. It means that sodium and calcium cations were attracted by the

336   negatively charged membrane and were highly distributed from the liquid phase to the

337   membrane phase. Chloride ions, which are much smaller than sulfate anions, tended to

338   pass through the membrane together with the cations in order to preserve the

339   electroneutrality (Hilal et al., 2015). Similar ion rejection behavior was observed by

340   Pérez-González et al. (2015), who treated brackish water desalination brines in the

341   pressure range of 5 to 20 bar using the same NF270 membrane. The observed ions

342   rejections were beneficial for increasing the conductivity of the concentrate to be used

343   as an electrolyte in the electrochemical treatment.

344   *3.1.2 Concentration mode experiments*

345   The purpose of the concentration mode experiments was to obtain a low volume

346   of highly concentrated PFHxA solution. In addition, these experiments allowed the

347   evaluation of the stability of membrane performance along the time of operation in

348   terms of PFHxA rejection and permeate flux. Fig. 5 shows the evolution of the permeate

349   flux over time (for samples S1 and S2) using a feed pressure of 10 bar. In both cases the

350   flux slightly decreased in the first hours and then stabilized at a constant value. The

351   membrane permeability values at constant flux were $L_{p,S1}$=9.4 L·m^{-2}·h^{-1}·bar^{-1} and

352    $L_{p,S2}$=8.6 L·m^{-2}·h^{-1}·bar^{-1}, which are similar or only slightly below those reported in the

353   above section. At the end of each experiment, the membrane was tested again with

354   ultrapure water to evaluate whether the observed loss of permeability corresponded to

355   reversible or irreversible fouling. For example, after the NF test with S1, the membrane

356   permeability to pure water was 12.8 L·m^{-2}·h^{-1}·bar^{-1}, which was only 4% less than the

357   initial value reported in Fig. 1. The difference is believed to be due to the variability of

358   properties in different membrane specimens. It was concluded that the NF of PFHxA

359   solutions did not generate irreversible fouling in the NF270 membrane.

360   In the concentration mode experiments, the NF270 membrane showed high

361   PFHxA real rejections that were essentially constant over time: 98.2 ± 0.2%, and 98.8 ±

362   0.2%, for S1 and S2 respectively (real and observed PFHXA rejection values with time

363   are compared in Figure S1 of the supplementary material). The volume was reduced

364   from the 10 L initially used as feed, to a final volume of approximately 2 L of

365   concentrate. PFHxA concentrations of 870 mg·L^{-1} and 344 mg·L^{-1} were achieved in the

366   final concentrates C-S1 and C-S2, respectively. The evolution with time of the PFHxA

367   concentration in retentate and permeate streams is given in Figure S2 of the

368   supplementary material. Simultaneously, the conductivity of the concentrates reached

369   2.48 mS·cm^{-1} and 2.63 mS·cm^{-1}. These concentrates served as feed for the next

370   electrooxidation step. PFHxA was detected in the permeates at concentrations of 21

371   mg·L^{-1} for S1, and 8 mg·L^{-1} for S2. These values corresponded to the composite

372   permeates obtained throughout the duration of the tests. Moreover, Fig. 6 shows that

373   under the conditions of the present study, PFHxA concentrations in the permeate and in

374   the retentate matched a linear relationship (r^2=0.97), an observation that further supports

375 diffusion as the predominant PFHxA transport mechanism through the NF270

376 membrane.

377 *3.2 Electrooxidation experiments*

378 *3.2.1 Influence of the applied current density*

379 Initial tests aimed at the selection of the applied current density were performed

380 using model solutions (CM-S1) that were prepared with similar PFHxA concentrations

381 and salts composition as the NF concentrates obtained from sample S1. Fig. 7 depicts

382 the development of PFHxA and TOC with time at three applied current density values:

383 J_{app}=20, 50, and 100 A·m^{-2}. The kinetics of PFHxA degradation and mineralization

384 were clearly enhanced when the applied current density was increased from 20 to 50

385 A·m^{-2}. Further increase in current density to 100 A·m^{-2} provided an additional

386 improvement in degradation kinetics, although less noticeable than in the previous jump

387 from 20 to 50 A·m^{-2}.

388 The recent review by Niu et al. (2016) proposed that electrochemical oxidation

389 mechanism of PFCAs involves electron transfer to the anode to form the highly reactive

390 $C_nF_{2n+1}COO^{\cdot}$ radical, which then reacts with electrogenerated hydroxyl radicals.

391 According to this pathway, PFHxA degradation would include both direct and indirect

392 electrochemical oxidation steps. BDD anodes are well known for their wide

393 electrochemical window that allows the formation of hydroxyl radicals at lower

394 electrode potentials than those needed for the oxygen evolution reaction. However, as

395 hydroxyl radicals are confined to the proximity of the anode surface, two different

396 operating regimes can be defined for BDD oxidation: i) when the applied current

397 density is below the limiting current density, the electrolysis is under current control

398 and the concentration of organic compounds decreases linearly with time; ii) when the

18

399 applied current density is above the limiting current density, the electrolysis is under

400 mass transport control and the removal of organics follows a first-order exponential

401 trend. In the present study, the limiting current density (J_{lim}, Eq. (3)) was calculated as

402 $J_{lim} = 48.1$ A·m^{-2} at the initial PFHxA concentration in CM-S1. This means that when

403 working at $J_{app} = 20$ A·m^{-2}, the electrolysis was initially under current control but

404 rapidly shifted to mass transfer control at t = 1 h as the concentration of PFHxA

405 decreased. When $J_{app} = 50$ A·m^{-2}, the system was working under mass transfer control

406 for the entire experiment. The small but noticeable increase in the PFHxA removal rate

407 observed at 100 A·m^{-2} can be assigned to the oxidative effect of secondary strong

408 oxidants such as sulfate radicals. This assumption is based on the results reported by

409 Hori et al. (2005), who found that the photolysis of persulfate anions produced highly

410 oxidative sulfate radical anions, which efficiently decomposed PFOA and other PFCAs

411 bearing C_4-C_8 perfluoroalkyl groups. At present, we are not able to definitely elucidate

412 the rate limiting step of PFHxA degradation, although the experimental results that

413 show only a minor kinetic enhancement when the applied current is doubled from 50 to

414 100 A·m^{-2}, point to the predominance of indirect oxidation by means of

415 electrogenerated oxidants.

416 To select the suitable operating conditions, it is also useful to look at the evolution of

417 PFHxA and TOC as functions of the specific electrical charge passed (Q), also shown in

418 Fig. 7. An increase in the applied current density did not significantly affect the efficacy

419 of the process. The energy demand for 90 % degradation of the initial PFHxA was

420 calculated using Eqs. (1) and (2). The times for 90% PFHxA reduction were obtained

421 from the rate constant calculated using the concentration-Q data. Results are

422 summarized in Table 2, where V is the experimental cell voltage developed under

423 galvanostatic conditions. The energy consumption for $J_{app} = 50$ A·m^{-2} was 15.2 kWh·m^{-3},

424 the lowest among the three current intensities under consideration. It was also observed

425 that the electrolysis time needed to reach 90 % degradation at 50 $A \cdot m^{-2}$ was three times

426 lower than when the applied current was 20 $A \cdot m^{-2}$. Accordingly, it was decided to select

427 J_{app}=50 $A \cdot m^{-2}$ as the working current density for the electrochemical treatment of the

428 real industrial process concentrates.

429 The energy consumption for the electrochemical treatment of PFHxA achieved in the

430 present study, 15.2 $kWh \cdot m^{-3}$, is lower than previously reported values for the removal of

431 different PFASs in waters. Zhuo et al. (2011) and Niu et al. (2012) reported the

432 electrolysis of PFOA using tin oxide and lead dioxide electrodes with energy

433 consumptions of 48 and 45 $kWh \cdot m^{-3}$. Similar values in the range 41.7-76.6 $kWh \cdot m^{-3}$

434 have been gathered by Niu et al. (2016) for the degradation of perfluorodecanoic and

435 perfluorononanoic acids using BDD, SnO_2, and PbO_2 electrodes. The energy

436 consumption reported in the present study is the lowest of all the values reported so far,

437 which shows evidence of the improvement of efficiency of the electrolysis treatment of

438 PFASs using a pre-concentration strategy.

439 *3.2.2 Electrochemical mineralization of PFHxA in concentrates from industrial process*

440 *waters.*

441 Fig. 8 shows the development of PFHxA and TOC when treating the real industrial

442 process waters pre-concentrated by NF at the selected value of current density (J_{app}=50

443 $A \cdot m^{-2}$). Linearized dimensionless values are presented, since the initial concentrations

444 of PFHxA in the two samples were significantly different. The volume of sample is

445 included in the linearization of data because of the lower feed water volume used for C-

446 S2 (0.8 L) than for C-S1 (1 L), due to the lack of sample. After 90 minutes, the

447 degradation of PFHxA concentration was 91% and 98% of the initial in samples C-S1

20

448 and C-S2, respectively. It is also interesting to confirm the high removal of TOC,

449 showing the mineralization of the organic compound. PFHxA removal was slightly

450 faster for C-S2 than for C-S1. This behavior can be assigned to its higher initial PFHxA

451 concentration ($C_{0,C-S1}$=870 mg·L^{-1}). During the experiments we detected degradation

452 products such as perfluoropentanoic acid and perfluorobutanoic acid. In all cases, the

453 observed amounts of secondary PFCAs were lower than the quantification limit of the

454 HPLC-DAD analytical technique. It means that only small amounts of the shorter chain

455 PFCAs obtained upon PFHxA degradation diffused out of the proximity of the anode

456 surface.

457 Fig. 9 shows the evolution of fluoride with electrochemical treatment. The fluoride

458 concentration reached a maximum at t = 90 min, and then started to decrease slowly. At

459 the same time, the concentration of calcium decreased continuously, a clear indication

460 that calcium fluoride was being formed from the beginning of the electrochemical test.

461 Local pH variations at the anode and cathode surfaces and the intense fluid turbulence

462 gave rise to the supersaturated calcium fluoride solution and deposition of calcium

463 fluoride on the cathode surface. For electrochemical treatment longer 2 h, the

464 degradation of PFHxA was nearly completed and there was no further release of

465 fluoride ions. The decrease of fluoride and calcium concentrations was contained

466 showing the slow precipitation of calcium fluoride. Therefore, in the present

467 application, defluorination rate is not an appropriate measurement of the degree of

468 mineralization of PFHxA, as that parameter takes into account the concentration of

469 fluoride ions in the solution. Calcium fluoride scaling was easily removed from the

470 cathode surface by acid cleaning using an aqueous solution of HCl (3 M) at the end of

471 each experimental run. This fouling formation could be detrimental to the performance

472 of the system at larger-scales, which would require implementing a periodical cleaning

21

473 procedure to avoid scaling on the electrode surface, as it was recently proposed by

474 Schaefer et al. (2016).

475 The pseudo-first order kinetic constant for PFHxA degradation obtained from the

476 experimental data in Fig. 8, was 0.0021 m·min^{-1}, after correcting for the volume treated

477 and anode area. This value is ten times higher than the kinetic constant obtained by Niu

478 et al. (2012) for the degradation of PFHxA using a Ce-doped PbO$_2$ anode. Similarly,

479 Zhuo et al. (2012) reported the electrooxidation of a synthetic aqueous solution of

480 PFHxA (100 mg·L^{-1}) using a small BDD anode (8.5 cm^2) in a laboratory-scale batch

481 reactor at an applied current of 232 A·m^{-2}. In that work, the reported PFHxA

482 degradation kinetic constant was 0.0016 m·min^{-1}. The kinetic constant obtained in the

483 present study surpasses the two previously reported values, and validates the use of

484 commercial BDD cells for the removal of PFASs from industrial process waters.

485 Fig. 10 shows an overview of the process that combines low pressure nanofiltration as

486 the preconcentration step, and electrooxidation as the degradation technique. This

487 strategy was able to eliminate 90% of the initial PFHxA mass contained in the industrial

488 process waters, at a moderate energy consumption, by increasing the concentration of

489 organic compounds for the electrooxidation process (Sirés et al., 2014). Higher removal

490 rates could be attained by using a more selective membrane system (such as reverse

491 osmosis) that however operates at higher pressures and provides much lower permeate

492 fluxes. Another option would be the electrochemical system alone, which would also be

493 able to further reduce the final PFHxA concentration, at the expense of a higher energy

494 consumption.

4. Conclusions

Results presented herein demonstrate that a combination of nanofiltration (NF) followed by the electrochemical oxidation (ELOX) of the NF concentrate is effective in removing perfluorohexanoic acid (PFHxA) from industrial process waters. Very few previous studies have reported the treatment of PFHxA, and none of them addressed the NF/ELOX conjunction or the concentration range found in industrial streams, thus showing the novelty of the present study.

It is concluded that the NF270 (Dow/Filmtech) membrane provides high PFHxA rejections (reaching 99.6% when operating at a feed pressure of 20 bar), without any noticeable membrane fouling. This performance improves on previously reported results with longer chain PFASs such as PFOA, which showed adhesion to the membrane that reduced the permeate flux. This implies that nanofiltration is a viable technical option for the separation of PFHxA from process water streams when compared to more extended adsorption practices. The presence of sulfate and the adequate rejection of divalent ions by the NF270 membrane provided adequate conductivity to the concentrate stream, which facilitated the subsequent application of electrochemical treatment without the further addition of electrolytes.

Electrooxidation with boron doped diamond electrodes, working at a current density of 50 A·m^{-2}, easily degraded the PFHxA retained in the NF concentrate. Traces of shorter chain PFASs were observed in the early stages of the electrochemical process, which nevertheless were later degraded below the limit of quantification of the analytical technique. The possible adverse impact of fluoride ions obtained as a final degradation product was avoided by in situ precipitation as calcium fluoride, promoted by the incoming calcium contained in the industrial process stream. The observed kinetics of

519   PFHxA oxidation was substantially faster than previously reported results using Ce-

520   doped PbO_2 and BDD anodes, probably fostered by the optimal selection of operation

521   variables achieved in this study.

522   Overall, these results suggest that the process integration of nanofiltration separation

523   and BDD electrochemical degradation is a promising alternative for the treatment of

524   PFHxA that could be extended to the treatment of waters impacted by other PFASs such

525   as PFOA and PFOS.

526

527   Funding

530

References

531   Ahrens, L., Bundschuh, M., 2014. Fate and effects of poly- and perfluoroalkyl

532

533   substances in the aquatic environment: A review. Environ. Toxicol. Chem. 33,

534   1921–1929.

535   Anglada, Á., Urtiaga, A., Ortiz, I., 2009. Contributions of electrochemical oxidation to

536   waste-water treatment: Fundamentals and review of applications. J. Chem.

537   Technol. Biotechnol. 84, 1747–1755. doi:10.1002/jctb.2214

538   Anglada, Á., Urtiaga, A.M., Ortiz, I., 2010. Laboratory and pilot plant scale study on

539   the electrochemical oxidation of landfill leachate. J. Hazard. Mater. 181, 729–735.

540   doi:10.1016/j.jhazmat.2010.05.073

541   Appleman, T.D., Dickenson, E.R. V, Bellona, C., Higgins, C.P., 2013. Nanofiltration

542   and granular activated carbon treatment of perfluoroalkyl acids. J. Hazard. Mater.

543   260, 740–746.

544   Appleman, T.D., Higgins, C.P., Quiñones, O., Vanderford, B.J., Kolstad, C., Zeigler-

545   Holady, J.C., Dickenson, E.R. V, 2014. Treatment of poly- and perfluoroalkyl

546   substances in U.S. full-scale water treatment systems. Water Res. 51, 246–255.

547   doi:http://dx.doi.org/10.1016/j.watres.2013.10.067

548   Arvaniti, O.S., Stasinakis, A.S., 2015. Review on the occurrence, fate and removal of

549   perfluorinated compounds during wastewater treatment. Sci. Total Environ. 524–

550   525, 81–92.

551   Asano, T., 1998. Wastewater Reclamation and Reuse: Water Quality Management

552   Library. CRC Press, Florida.

553 Baudequin, C., Mai, Z., Rakib, M., Deguerry, I., Severac, R., Pabon, M., Couallier, E.,

554   2014. Removal of fluorinated surfactants by reverse osmosis - Role of surfactants

555   in membrane fouling. J. Memb. Sci. 458, 111–119.

556   doi:10.1016/j.memsci.2014.01.063

557 Bellona, C., Drewes, J.E., 2007. Viability of a low-pressure nanofilter in treating

558   recycled water for water reuse applications: A pilot-scale study. Water Res. 41,

559   3948–3958. doi:10.1016/j.watres.2007.05.027

560 Cabeza, A., Urtiaga, A.M., Ortiz, I., 2007. Electrochemical treatment of landfill

561   leachates using a boron-doped diamond anode. Ind. Eng. Chem. Res. 46, 1439–

562   1446. doi:10.1021/ie061373x

563 Cañizares, P., Lobato, J., Paz, R., Rodrigo, M.A., Sáez, C., 2005. Electrochemical

564   oxidation of phenolic wastes with boron-doped diamond anodes. Water Res. 39,

565   2687–2703. doi:10.1016/j.watres.2005.04.042

566 Carter, K.E., Farrell, J., 2008. Oxidative destruction of perfluorooctane sulfonate using

567   boron-doped diamond film electrodes. Environ. Sci. Technol. 42, 6111–6115.

568   doi:10.1021/es703273s

569 Chaplin, B.P., 2014. Critical review of electrochemical advanced oxidation processes

570   for water treatment applications. Environ. Sci. Process. Impacts 16, 1182–1203.

571   doi:10.1039/c3em00679d

572 Dialynas, E., Mantzavinos, D., Diamadopoulos, E., 2008. Advanced treatment of the

573   reverse osmosis concentrate produced during reclamation of municipal wastewater.

574   Water Res. 42, 4603–4608. doi:10.1016/j.watres.2008.08.008

575   Díaz, V., Ibáñez, R., Gómez, P., Urtiaga, A.M., Ortiz, I., 2011. Kinetics of electro-

576   oxidation of ammonia-N, nitrites and COD from a recirculating aquaculture saline

577   water system using BDD anodes. Water Res. 45, 125–134.

578   doi:http://dx.doi.org/10.1016/j.watres.2010.08.020

579   ECHA, 2014. Candidate list of substances of very high concern for authorisation

580   [WWW Document]. URL https://echa.europa.eu/candidate-list-table

581   Fujioka, T., Nghiem, L.D., Khan, S.J., McDonald, J.A., Poussade, Y., Drewes, J.E.,

582   2012. Effects of feed solution characteristics on the rejection of N-nitrosamines by

583   reverse osmosis membranes. J. Memb. Sci. 409–410, 66–74.

584   doi:10.1016/j.memsci.2012.03.035

585   Hang, X., Chen, X., Luo, J., Cao, W., Wan, Y., 2015. Removal and recovery of

586   perfluorooctanoate from wastewater by nanofiltration. Sep. Purif. Technol. 145,

587   120–129.

588   Hilal, N., Kochkodan, V., Al Abdulgader, H., Johnson, D., 2015. A combined ion

589   exchange-nanofiltration process for water desalination: II. Membrane selection.

590   Desalination 363, 51–57. doi:10.1016/j.desal.2014.11.017

591   Hori, H., Yamamoto, A., Hayakawa, E., Taniyasu, S., Yamashita, N., Kutsuna, S.,

592   Kiatagawa, H., Arakawa, R., 2005. Efficient decomposition of environmentally

593   persistent perfluorocarboxylic acids by use of persulfate as a photochemical

594   oxidant. Environ. Sci. Technol. 39. doi:10.1021/es0484754

595   Ioannou, L.A., Michael, C., Vakondios, N., Drosou, K., Xekoukoulotakis, N.P.,

596   Diamadopoulos, E., Fatta-Kassinos, D., 2013. Winery wastewater purification by

597   reverse osmosis and oxidation of the concentrate by solar photo-Fenton. Sep. Purif.

27

598   Technol. 118, 659–669. doi:10.1016/j.seppur.2013.07.049

599   IUPAC, 1996. Terminology for membranes and membrane processes (IUPAC

600   Recommendation 1996). J. Memb. Sci. 120, 149–159. doi:10.1016/0376-

601   7388(96)82861-4

602   Lin, A.Y.C., Panchangam, S.C., Tsai, Y.T., Yu, T.H., 2014. Occurrence of

603   perfluorinated compounds in the aquatic environment as found in science park

604   effluent, river water, rainwater, sediments, and biotissues. Environ. Monit. Assess.

605   186, 3265–3275. doi:10.1007/s10661-014-3617-9

606   Martínez-Huitle, C.A., Rodrigo, M.A., Sirés, I., Scialdone, O., 2015. Single and

607   Coupled Electrochemical Processes and Reactors for the Abatement of Organic

608   Water Pollutants: A Critical Review. Chem. Rev. 115, 13362–13407.

609   doi:10.1021/acs.chemrev.5b00361

610   Mulder, M., 1996. Basic Principles of Membrane Technology, Zeitschrift für

611   Physikalische Chemie. Springer, Netherlands.

612   doi:10.1524/zpch.1998.203.Part_1_2.263

613   Nghiem, L.D., Hawkes, S., 2007. Effects of membrane fouling on the nanofiltration of

614   pharmaceutically active compounds (PhACs): Mechanisms and role of membrane

615   pore size. Sep. Purif. Technol. 57, 176–184.

616   doi:http://dx.doi.org/10.1016/j.seppur.2007.04.002

617   Niu, J., Li, Y., Shang, E., Xu, Z., Liu, J., 2016. Electrochemical oxidation of

618   perfluorinated compounds in water. Chemosphere 146, 526–538.

619   doi:10.1016/j.chemosphere.2015.11.115

620 Niu, J., Lin, H., Xu, J., Wu, H., Li, Y., 2012. Electrochemical mineralization of

621   perfluorocarboxylic acids (PFCAs) by Ce-doped modified porous nanocrystalline

622   PbO2 film electrode. Environ. Sci. Technol. 46, 10191–10198.

623   doi:10.1021/es302148z

624 Ochiai, T., Iizuka, Y., Nakata, K., Murakami, T., Tryk, D.A., Fujishima, A., Koide, Y.,

625   Morito, Y., 2011. Efficient electrochemical decomposition of perfluorocarboxylic

626   acids by the use of a boron-doped diamond electrode. Diam. Relat. Mater. 20, 64–

627   67. doi:10.1016/j.diamond.2010.12.008

628 Panizza, M., Cerisola, G., 2009. Direct and mediated anodic oxidation of organic

629   pollutants. Chem. Rev. 109, 6541–6569. doi:10.1021/cr9001319

630 Pérez-González, A., Ibáñez, R., Gómez, P., Urtiaga, A.M., Ortiz, I., Irabien, J.A., 2015.

631   Nanofiltration separation of polyvalent and monovalent anions in desalination

632   brines. J. Memb. Sci. 473, 16–27.

633   doi:http://dx.doi.org/10.1016/j.memsci.2014.08.045

634 Pérez, G., Fernández-Alba, A.R., Urtiaga, A.M., Ortiz, I., 2010. Electro-oxidation of

635   reverse osmosis concentrates generated in tertiary water treatment. Water Res. 44,

636   2763–2772. doi:http://dx.doi.org/10.1016/j.watres.2010.02.017

637 Perry, R.H., Green, D.W., Maloney, J.O., 1997. Perry's Chemical Engineers'

638   Handbook, Chemical Engineering Series. McGraw-Hill Professional Publishing,

639   New York.

640 Polcaro, A.M., Vacca, A., Mascia, M., Palmas, S., Rodriguez Ruiz, J., 2009.

641   Electrochemical treatment of waters with BDD anodes: Kinetics of the reactions

642   involving chlorides. J. Appl. Electrochem. 39, 2083–2092. doi:10.1007/s10800-

643   009-9870-x

644   Radjenovic, J., Bagastyo, A., Rozendal, R.A., Mu, Y., Keller, J., Rabaey, K., 2011.

645   Electrochemical oxidation of trace organic contaminants in reverse osmosis

646   concentrate using RuO2/IrO2-coated titanium anodes. Water Res. 45, 1579–1586.

647   doi:http://dx.doi.org/10.1016/j.watres.2010.11.035

648   Rahman, M.F., Peldszus, S., Anderson, W.B., 2014. Behaviour and fate of

649   perfluoroalkyl and polyfluoroalkyl substances (PFASs) in drinking water

650   treatment: A review. Water Res. 50, 318–340.

651   Samson, E., Marchand, J., Snyder, K.A., 2003. Calculation of ionic diffusion

652   coefficients on the basis of migration test results. Mater. Struct. Constr. 36, 156–

653   165. doi:10.1617/14002

654   Sansotera, M., Persico, F., Pirola, C., Navarrini, W., Di Michele, A., Bianchi, C.L.,

655   2014. Decomposition of perfluorooctanoic acid photocatalyzed by titanium

656   dioxide: Chemical modification of the catalyst surface induced by fluoride ions.

657   Appl. Catal. B Environ. 148, 29–35. doi:10.1016/j.apcatb.2013.10.038

658   Schaefer, C.E., Andaya, C., Urtiaga, A., McKenzie, E.R., Higgins, C.P., 2015.

659   Electrochemical treatment of perfluorooctanoic acid (PFOA) and perfluorooctane

660   sulfonic acid (PFOS) in groundwater impacted by aqueous film forming foams

661   (AFFFs). J. Hazard. Mater. 295, 170–175. doi:10.1016/j.jhazmat.2015.04.024

662   Schaefer, C.E., Lavorgna, G.M., Webster, T.S., Deshusses, M.A., Andaya, C., Urtiaga,

663   A., 2016. Pilot-scale electrochemical disinfection of surface water: assessing

664   disinfection by-product and free chlorine formation. Water Sci. Technol. Water

665   Supply.

666   Sirés, I., Brillas, E., Oturan, M.A., Rodrigo, M.A., Panizza, M., 2014. Electrochemical

667   advanced oxidation processes: Today and tomorrow. A review. Environ. Sci.

668   Pollut. Res. 21, 8336–8367. doi:10.1007/s11356-014-2783-1

669   Steinle-Darling, E., Reinhard, M., 2008. Nanofiltration for trace organic contaminant

670   removal: Structure, solution, and membrane fouling effects on the rejection of

671   perfluorochemicals. Environ. Sci. Technol. 42, 5292–5297.

672   Tang, C.Y., Fu, Q.S., Criddle, C.S., Leckie, J.O., 2007. Effect of Flux (Transmembrane

673   Pressure) and Membrane Properties on Fouling and Rejection of Reverse Osmosis

674   and Nanofiltration Membranes Treating Perfluorooctane Sulfonate Containing

675   Wastewater. Environ. Sci. Technol. doi:10.1021/es062052f

676   Tang, C.Y., Fu, Q.S., Robertson, A.P., Criddle, C.S., Leckie, J.O., 2006. Use of Reverse

677   Osmosis Membranes to Remove Perfluorooctane Sulfonate (PFOS) from

678   Semiconductor Wastewater. Environ. Sci. Technol. doi:- 10.1021/es060831q

679   Urtiaga, A., Fernández-González, C., Gómez-Lavín, S., Ortiz, I., 2015. Kinetics of the

680   electrochemical mineralization of perfluorooctanoic acid on ultrananocrystalline

681   boron doped conductive diamond electrodes. Chemosphere 129, 20–26.

682   doi:10.1016/j.chemosphere.2014.05.090

683   Urtiaga, A., Gómez, P., Arruti, A., Ortiz, I., 2014. Electrochemical removal of

684   tetrahydrofuran from industrial wastewaters: Anode selection and process scale-up.

685   J. Chem. Technol. Biotechnol. 89, 1243–1250. doi:10.1002/jctb.4384

686   USEPA, 2016. Drinking Water Health Advisories for PFOA and PFOS [WWW

687   Document]. URL https://www.epa.gov/ground-water-and-drinking-water/drinking-

688   water-health-advisories-pfoa-and-pfos

689   USEPA, 2015. Fact Sheet: 2010/2015 PFOA Stewardship Program [WWW Document].

690   URL https://www.epa.gov/assessing-and-managing-chemicals-under-tsca/fact-

691   sheet-20102015-pfoa-stewardship-program#meet

692   van den Berg, G.B., Rácz, I.G., Smolders, C.A., 1989. Mass transfer coefficients in

693   cross-flow ultrafiltration. J. Memb. Sci. 47, 25–51.

694   doi:http://dx.doi.org/10.1016/S0376-7388(00)80858-3

695   Wang, J., Wang, Z., Liu, Y., Wang, J., Wang, S., 2016. Surface modification of NF

696   membrane with zwitterionic polymer to improve anti-biofouling property. J.

697   Memb. Sci. 514, 407–417. doi:10.1016/j.memsci.2016.05.014

698   Wang, T., Zhao, C., Li, P., Li, Y., Wang, J., 2015. Fabrication of novel poly(m-

699   phenylene isophthalamide) hollow fiber nanofiltration membrane for effective

700   removal of trace amount perfluorooctane sulfonate from water. J. Memb. Sci. 477,

701   74–85. doi:http://dx.doi.org/10.1016/j.memsci.2014.12.038

702   Wang, Z., Cousins, I.T., Scheringer, M., Hungerbuehler, K., 2015. Hazard assessment

703   of fluorinated alternatives to long-chain perfluoroalkyl acids (PFAAs) and their

704   precursors: Status quo, ongoing challenges and possible solutions. Environ. Int. 75,

705   172–179. doi:10.1016/j.envint.2014.11.013

706   Xue, A., Yuan, Z.W., Sun, Y., Cao, A.Y., Zhao, H.Z., 2015. Electro-oxidation of

707   perfluorooctanoic acid by carbon nanotube sponge anode and the mechanism.

708   Chemosphere 141, 120–126. doi:10.1016/j.chemosphere.2015.06.095

709   Yang, B., Jiang, C., Yu, G., Zhuo, Q., Deng, S., Wu, J., Zhang, H., 2015. Highly

710   efficient electrochemical degradation of perfluorooctanoic acid (PFOA) by F-

711   doped Ti/SnO2 electrode. J. Hazard. Mater. 299, 417–424.

712   doi:10.1016/j.jhazmat.2015.06.033

713   Yu, Q., Zhang, R., Deng, S., Huang, J., Yu, G., 2009. Sorption of perfluorooctane

714   sulfonate and perfluorooctanoate on activated carbons and resin: Kinetic and

715   isotherm study. Water Res. 43, 1150–1158.

716   doi:http://dx.doi.org/10.1016/j.watres.2008.12.001

717   Zaggia, A., Conte, L., Falletti, L., Fant, M., Chiorboli, A., 2016. Use of strong anion

718   exchange resins for the removal of perfluoroalkylated substances from

719   contaminated drinking water in batch and continuous pilot plants. Water Res. 91,

720   137–146. doi:http://dx.doi.org/10.1016/j.watres.2015.12.039

721   Zhang, D., Luo, Q., Gao, B., Chiang, S.Y.D., Woodward, D., Huang, Q., 2016. Sorption

722   of perfluorooctanoic acid, perfluorooctane sulfonate and perfluoroheptanoic acid

723   on granular activated carbon. Chemosphere 144, 2336–2342.

724   doi:10.1016/j.chemosphere.2015.10.124

725   Zhao, C., Zhang, J., He, G., Wang, T., Hou, D., Luan, Z., 2013. Perfluorooctane

726   sulfonate removal by nanofiltration membrane the role of calcium ions. Chem.

727   Eng. J. 233, 224–232. doi:http://dx.doi.org/10.1016/j.cej.2013.08.027

728   Zhao, H., Gao, J., Zhao, G., Fan, J., Wang, Y., Wang, Y., 2013. Fabrication of novel

729   SnO2-Sb/carbon aerogel electrode for ultrasonic electrochemical oxidation of

730   perfluorooctanoate with high catalytic efficiency. Appl. Catal. B Environ. 136,

731   278–286. doi:10.1016/j.apcatb.2013.02.013

732   Zhao, L., Folsom, P.W., Wolstenholme, B.W., Sun, H., Wang, N., Buck, R.C., 2013.

733   6:2 Fluorotelomer alcohol biotransformation in an aerobic river sediment system.

734   Chemosphere 90, 203–209. doi:10.1016/j.chemosphere.2012.06.035

735   Zhuo, Q., Deng, S., Yang, B., Huang, J., Wang, B., Zhang, T., Yu, G., 2012.

736   Degradation of perfluorinated compounds on a boron-doped diamond electrode.

737   Electrochim. Acta 77, 17–22. doi:10.1016/j.electacta.2012.04.145

738   Zhuo, Q., Deng, S., Yang, B., Huang, J., Yu, G., 2011. Efficient electrochemical

739   oxidation of perfluorooctanoate using a Ti/SnO2-Sb-Bi anode. Environ. Sci.

740   Technol. 45, 2973–2979. doi:10.1021/es1024542

741   Zhuo, Q., Li, X., Yan, F., Yang, B., Deng, S., Huang, J., Yu, G., 2014. Electrochemical

742   oxidation of 1H,1H,2H,2H-perfluorooctane sulfonic acid (6:2 FTS) on DSA

743   electrode: Operating parameters and mechanism. J. Environ. Sci. 26, 1733–1739.

744   doi:10.1016/j.jes.2014.06.014

745

746

747

748

749

Captions

List of tables captions

Table 1. Main characteristics of the industrial process water samples used in the

experimental study

Table 2. Energy consumption and electrolysis time required to achieve 90%

PFHxAdegradation in sample CM-S1.

756

List of figures captions

Figure 1. Nanofiltration set-up in a) total recirculation mode, and b) concentration

mode.

Figure 2. Experimental permeate flux data as a function of the effective pressure

gradient. Model solution composition: NaCl (60 mg·L^{-1}), CaSO$_4$ (600 mg·L^{-1}).

Averages of duplicate experiments are reported for ultrapure water and the model

solution.

Figure 3. PFHxA real rejection as a function of the effective pressure for process water

samples S1 and S2 using an NF270 membrane.

Figure 4. Real rejection of ions as a function of the effective pressure. Data were

obtained using sample S1 and an NF270 membrane. Similar results were observed for

S2 sample and the model solution.

769   **Figure 5.** Nanofiltration operation in concentration mode. Permeate flux evolution with

770   time for samples S1 and S2. Feed pressure = 10 bar.

771   **Figure 6.** Nanofiltration operation in concentration mode. PFHxA concentration in the

772   permeate vs. PFHxA concentration in the retentate. The NF270 membrane was operated

773   at a feed pressure of 10 bar.

774   **Figure 7.** PFHxA and TOC evolution as function of time (t) and specific electrical

775   charge (Q), using the NF concentrate of sample S1: CM-S1 $[PFHxA]_0$=774 mg·L^{-1}; C-

776   S1 $[PFHxA]_0$=870 mg·L^{-1}. Initial conductivity=2.31-24.48 mS·cm^{-1}. ♦: J=20 A·m^{-2}; ■: J

777   =50 A·m^{-2}; ▲: J =100 A·m^{-2}.

778   **Figure 8.** Linearized dimensionless PFHxA and TOC evolution with time using the real

779   concentrates. J_{app}=50 A·m^{-2}. ♦:C-S1, $[PFHxA]_0$=870 mg·L^{-1}, initial conductivity = 2.48

780   mS·cm^{-1}, volume=1 L; ●:C-S2, $[PFHxA]_0$=344 mg·L^{-1}, initial conductivity = 2.63

781   mS·cm^{-1}, volume=0.8 L.

782   **Figure 9.** Calcium and fluoride evolution during the electrochemical treatment of

783   sample C-S1.

784   **Figure 10.** Global scheme of the combined NF- electrooxidation process.

36

Table 1. Main characteristics of the industrial process water samples used in the experimental study
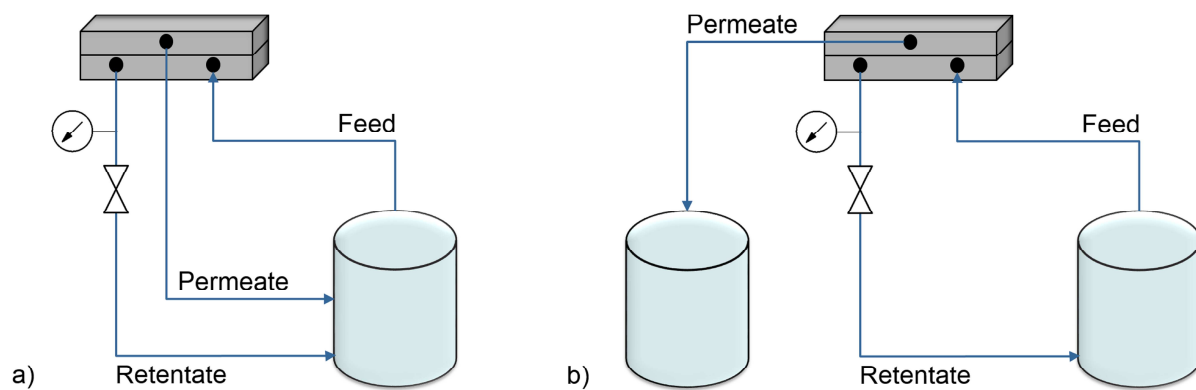
Parameter	Units	Sample	
		S1	S2
PFHxA	mg·L^{-1}	204	64
TOC	mg·L^{-1}	82	24
pH	-	7.7	7.4
Conductivity	mS·cm^{-1}	1.05	1.02
Chloride	mg·L^{-1}	19.8	16.9
Sulfate		321	360
Bicarbonate		98	92
Calcium		172	171
Sodium		24.9	28.7

Table 2. Energy consumption and electrolysis time required to achieve 90%

PFHxAdegradation in sample CM-S1.

J_{app} (A·m^{-2})	Kinetic constant k_2 (h^{-1})*	V (V)	Q (A·h·L^{-1})	W (kWh·m^{-3})	Electrolysis time (h)
20	1.859	12.9	1.24	16.0	4.42
50	2.252	14.9	1.02	15.2	1.47
100	1.814	16.8	1.27	21.3	0.90

* k_2 obtained from the fitting of experimental concentration vs. Q data to $[PFHxA]/[PFHxA]_0=e^{(-k2.Q)}$

Feed

Permeate

Retentate

a)

Permeate

Feed

Retentate

b)

10 L

S1: 204 mg L^{-1}
S2: 64 mg L^{-1}

Nanofiltration

2 L

S1: 870 mg L^{-1}
S2: 344 mg L^{-1}

Electrooxidation

S1: 37 mg L^{-1}
S2: 2 mg L^{-1}

8 L

S1: 21 mg L^{-1}
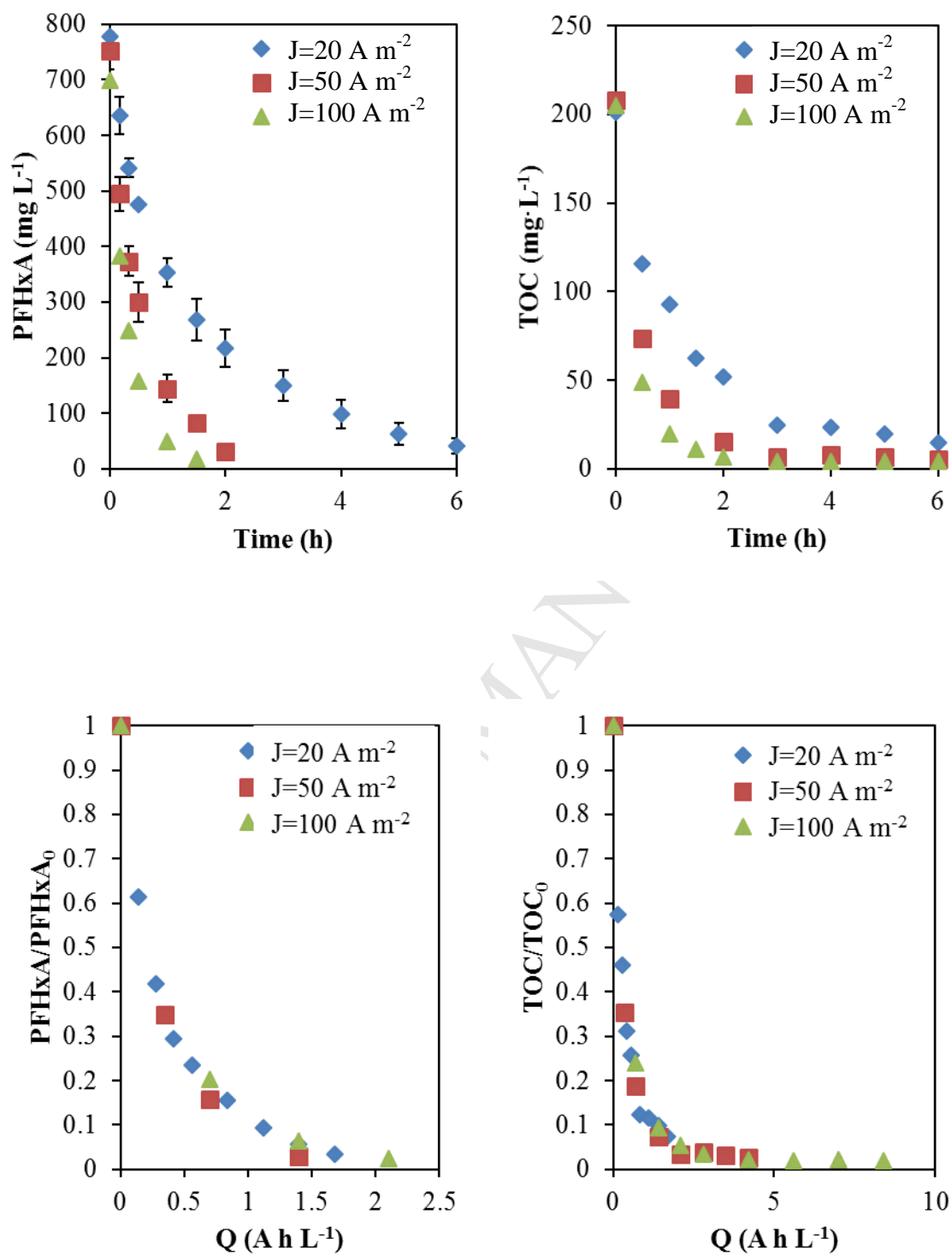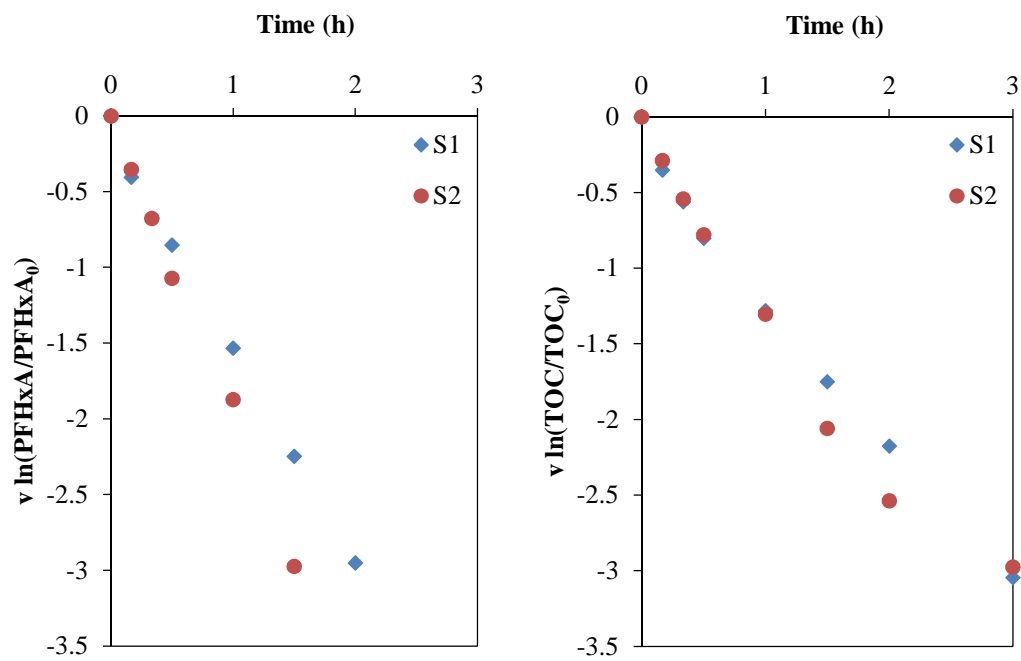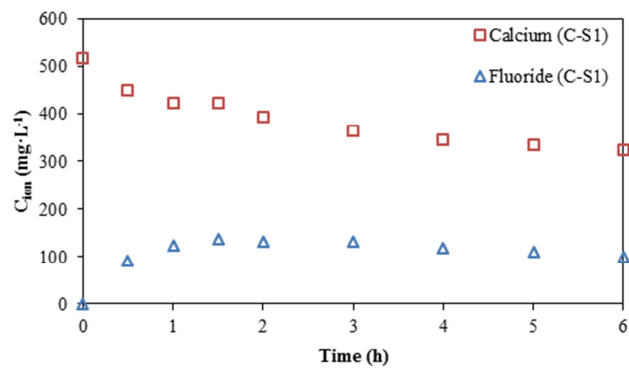S2: 8 mg L^{-1}
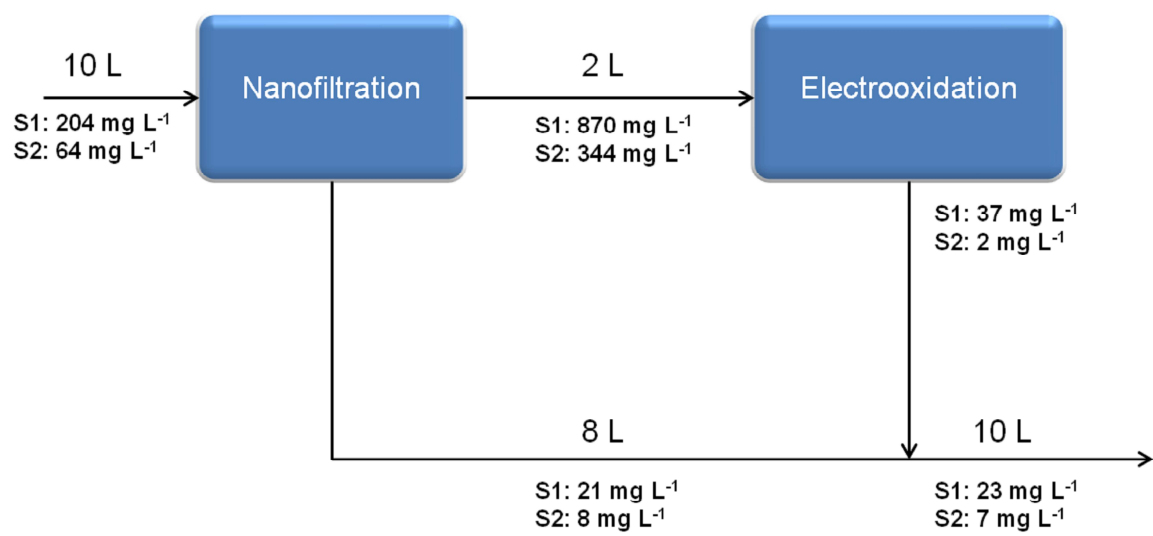
10 L

S1: 23 mg L^{-1}
S2: 7 mg L^{-1}
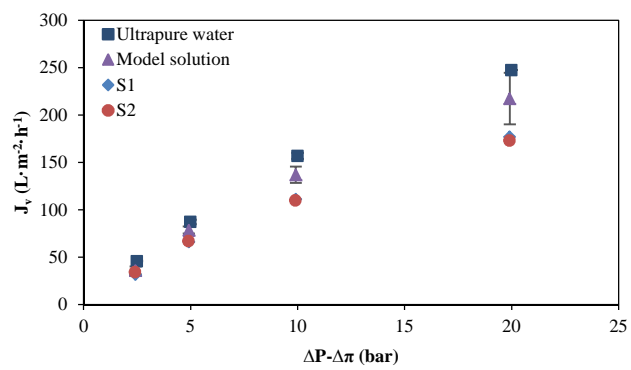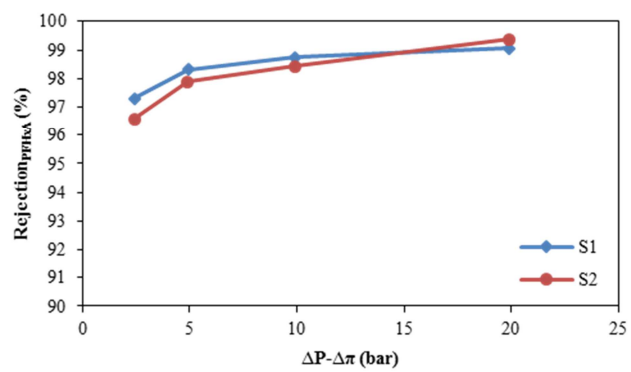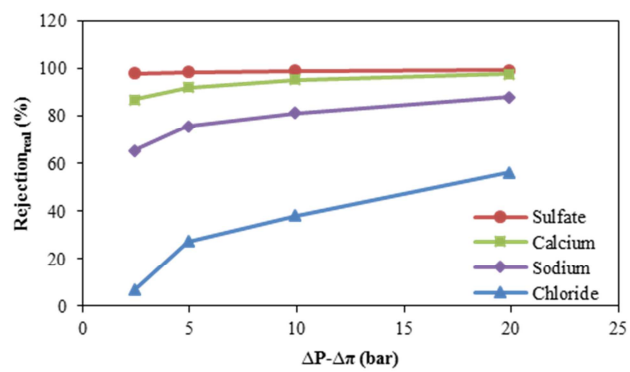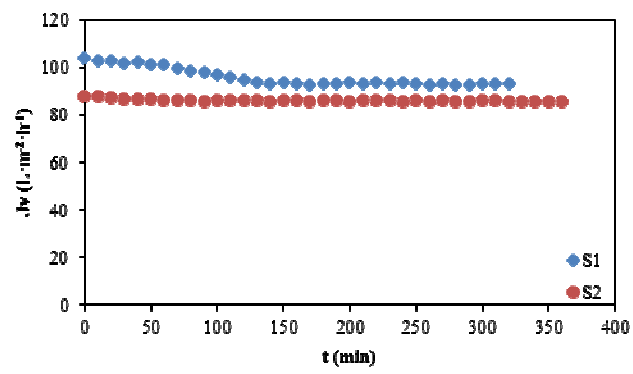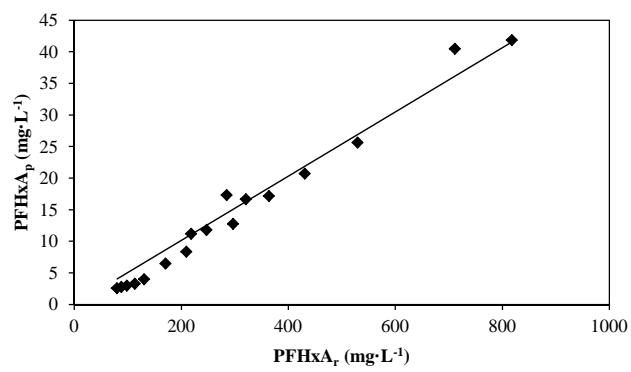
- A combined nanofiltration/electrooxidation process was used to eliminate PFHxA for the first time
- Real industrial process waters were treated.
- NF270 membranes showed PFHxA rejection that reached 99.6% without membrane fouling.
- 98% of PFHxA in the NF concentrate was degraded by BDD electrodes. Mineralization > 95% was achieved
- Electrochemical conditions were optimized for minimizing the energy consumption.